(Br)₂BODIPY Photosensitizers: Influence of Functionalization Features on Photophysical, Photochemical Characteristics and Aggregation Behavior in Solutions

Sofya A. Dogadaeva,[a@] Alexander A. Kalyagin,[a] Alexander A. Ksenofontov,[a]
Lubov A. Antina,[a] Mikhail B. Berezin,[a] Elena V. Antina,[a] and Alexander S. Semeikin[b]

[a]Institute of Solution Chemistry of Russian Academy of Sciences, 153045 Ivanovo, Russia
[b]Ivanovo State University of Chemistry and Technology, 153000 Ivanovo, Russia
[@]Corresponding author E-mail: sonya_dogadaeva@mail.ru

The synthesis of low-toxic photosensitizers with an optimal ratio of fluorescence and singlet oxygen generation intensity (theranostics) is an urgent task. Dipyrromethene difluoroborates (BODIPYs) occupy a significant place in this area of research. We present the results of the synthesis, structural analysis, study of the chromophore, fluorescent and generation characteristics of BODIPYs, substituted with bromine atoms at the α,α-, β,β- and β',β'- positions of the molecule, their photo- and thermal stability, as well as the features of aggregation behavior in a mixed solvent THF–water. The results obtained were analyzed in comparison with non-halogenated compounds. It has been established that the introduction of bromine atoms into the BODIPY molecule quenches the fluorescent intensity and enhances the singlet oxygen generation. (α-Br)₂- and (β-Br)₂-substituted BODIPYs can be considered as potential theranostics with a predominant bioimaging function, while (β'-Br)₂-BODIPY exhibits a photosensitizer function to a greater extent. Symmetric bromination of BODIPY has a little effect on photo- and thermal stability compared to unsubstituted analogues. The studied bromine substituted boron(III) dipyrromethenates are characterized by the formation of non-fluorescent H-aggregates in a mixed THF-water solvent with a water content in the mixture above 70%.

Keywords: Dibromosubstituted BODIPY, photosensitizer, fluorescence, singlet oxygen generation, photostability, thermal stability, aggregation.

(Br)₂BODIPY фотосенсибилизаторы: влияние особенностей функционализации на фотофизические, фотохимические характеристики и агрегационное поведение в растворах

С. А. Догадаева,[a@] А. А. Калягин,[a] А. А. Ксенофонтов,[a] Л. А. Антина,[a]
М. Б. Березин,[a] Е. В. Антина,[a] А. С. Семейкин[b]

[a]Институт химии растворов им. Г.А. Крестова РАН, 153045 Иваново, Россия
[b]Ивановский государственный химико-технологический университет, 153000 Иваново, Россия
[@]E-mail: sonya_dogadaeva@mail.ru

Синтез малотоксичных фотосенсибилизаторов с оптимальным соотношением интенсивности флуоресценции и генерации синглетного кислорода (тераностиков) является актуальной задачей. В этой области исследований дифторбораты дипиррометенов (BODIPY) занимают существенное место. Нами представлены результаты синтеза, анализа строения, изучения хромофорных, флуоресцентных и генерационных характеристик BODIPY, замещенных атомами брома в α,α-, β,β- и β',β'- положениях, их фото-, термостабильности, а также особенностей агрегационного поведения в смешанном растворителе ТГФ–вода. Полученные результаты проанализированы в сравнении с негалогенированными соединениями. Установлено, что введение атомов брома в молекулу тушит флуоресцентные, но усиливает генерационные свойства BODIPY. (α-Br)₂- и (β-Br)₂-замещенные BODIPY можно рассматривать как потенциальные тераностики с преобладанием

функции биовизуализатора, а (β'-Br)₂-BODIPY в большей степени проявляет функцию фотосенсибилизатора. Симметричное бромирование BODIPY незначительно влияет на фото- и термическую стабильность по сравнению с незамещенными аналогами. Исследованные бромзамещенные дипирpрометенаты бора(III) характеризуются образованием нефлуоресцирующих H-агрегатов в смешанном растворителе ТГФ-вода при содержании воды в смеси более 70%.

Introduction

To date, no one in the scientific world has any doubt that porphyrins are non-trivial molecules. Composition, complex and changeable geometric and electronic structure combining different possibilities for interaction with environment (matter and field) provide porphyrins with a variety of biological functions and application in various fields of science and technology.[1,2] Dipyrromethenes are porphyrins precursors. They offer no less pronounced set of practically significant properties. Increased scientific interest in these compounds arose after the publication of the monograph (H. Falk, 1989) where promising research results in the field of oligopyrrole pigments chemistry were summarized.[3] Fundamental ideas about feature of physicochemical properties of dipyrromethene ligands, salts and coordination compounds formed over the past years became a base for development actual modern direction of practical application of oligopyrrole compounds and luminophores as sensors, markers, agents for photodynamic therapy (PDT) *etc*.[4]

Coordination compounds of boron(III) with dipyrromethenes (BODIPY) took the one of the most promising and actively studied positions among the majority of known luminophores by now. The field of BODIPY application is actively expanding. Today it covers such different ways as sensors,[5–8] biomarkers,[9] drug delivery systems, PDT agents,[10] antibacterial, antimicrobial and antifungal agents,[11–13] fluorescent switches,[9] laser dyes,[14–16] *etc*. The main advantages of these luminophores are high fluorescence quantum yields, intense absorption profile, good photo- and thermal stability.[17–20]

Nowadays because of active use of PDT techniques for the diagnosis and treatment of oncological diseases, biocompatible theranostic agents are needed. For complex functionality – imaging and destruction of tumor such agents should possess minimal possible dark cytotoxicity, high affinity for tumor cells, optimal combination of fluorescent and generation characteristics. To combine fluorescent diagnostics (FD) and photodynamic therapy into simple biocompatible system with one chromophore component is not easy. The generation of singlet oxygen and/or free radical and fluorescence are competing processes in the exited state of the photosensitizer (PS). For theranostics both key properties must be successfully balanced. Therefore, development of new photodiagnostic tools combining optimal fluorescence and singlet oxygen generation is one of in-demand and difficult tasks for modern preparative chemistry and biomedicine.

Boron(III) dipyrromethenates are of significant interest for the development of PDT agents or theranostics. To date, halogen-substituted BODIPYs are proposed as prom-ising effective agents for photodynamic therapy. Structural similarity to porphyrins provides them with biocompatibility and minimal dark toxicity.[21] Also BODIPYs are characterized by high photostability, the ability to effectively penetrate the lipid layers of cell membranes and affinity for tumor tissues.

In this work the influence of the α,α-, β,β- or β′,β′-positions bromination features of the boron(III) dipyrromethenates pyrrole nuclei on their photophysical, photochemical characteristics and aggregation behavior in solutions are considered, the possibility of their use as potential theranostic agents for PDT is estimated.

Experimental

Computational modeling

All calculation were carried out Gaussian 16, Revision C.01 program package.[22] The geometries of dibromosubstituted BODIPY **1-3** (Figure 1) were optimized using a ωB97X-D/aug-cc-pVDZ.[23,24] Energy minima of optimized geometry were confirmed by absence of the imaginary frequencies. The vertical electronic transition energies were computed by the TDDFT method, employing CAMB3LYP/aug-cc-pVDZ.[25] The solvent effect (DCM) was modeled using the CPCM.[26] The ChemCraft 1.8 was used to analyze the results and molecular graphics.[27]

Characterization

The ¹H NMR spectra of compounds in deuterated chloroform (CDCl₃) were obtained using AVANCE-500 NMR spectrometer (Bruker, Germany) with operating frequency 500 MHz (TMS is an internal standard).

Electronic absorption spectra (EAS) of solutions were recorded using SF-56 spectrophotometer (LOMO, Russia) in the spectral range 300–700 nm. The studies were carried out in quartz cuvettes (l = 1 cm). The fluorescence spectra were obtained under the same conditions using CM 2203 spectrofluorimeter (SOLAR, Belarus) at an optical density and an excitation wavelength (490–500 nm) not exceeding 0.1. A solution of Rhodamine 6G in ethanol (Φ_{fl} = 0.94) was used as a standard for determining the relative fluorescence quantum yield (Φ_{fl}).[28] Stokes shift was determined as the difference of fluorescence and absorption intensity maxima wavelengths. MALDI TOF mass spectra were recorded on a Shimadzu AXIMA Confidence MALDI TOF mass spectrometer in positive ion reflection mode.

The fluorescence lifetime were obtained according to known methodology.[29–31] Measurements were carried out by means of time-resolved FluoTime 300 (PicoQuant) spectrometer with a laser LDH-P-C-500 (PicoQuant) as an excitation source. The instrument response function (IRF) was measured with the stray light signal of the dilute colloidal silica suspension (LUDOX®). The fluorescence decay curves measured, fluorescence lifetime were obtained by reconvolution of the decay curves using the EasyTau 2 software package (PicoQuant, Germany).

The singlet oxygen quantum yield (Φ_Δ) was determined from phosphorescence characteristics at 1275 nm: phosphorescence spectra and lifetime of $^1O_2$. The data were obtained by using FluoTime 300 (PicoQuant) spectrometer with a laser LDH-P-C-500 (PicoQuant) as an excitation source. Bengal rose (BR) and tetraphenylporphine (TPP) solutions with known Φ_Δ values[32–36] in the corresponding solvents were used as standarts.

To investigate comparative photostability solutions of boron(III) dipyrromethenates **1-3**, **1a-3a** (Figure 1) were prepared in cyclohexane and benzene with concentration ~2·10⁻⁵ mol L⁻¹. The quartz cuvette with solution was placed into thermostatic compartment (25±0.1 °C) with UV LED emitter (λ = 365 nm). Specific lighting power (W_{365}) was 3.5 W/m² (UV power meter LH-106) at the cuvette installation point. EAS of solution was recorded at regular intervals of irradiation (from 5 to 30 min) at the wavelength range 350–600 nm. The half-life ($\tau_{1/2}$) was defined as time during which complex is destructed by 50% at the absorption band maximum. Calculation of the photodestruction observed constant (k_{obs}) was carried out according to the equation[37, 38] based on Bouguer-Lambert-Beer law.

Thermogravimetric analysis (TG/DTG) of the complexes was carried out by means of Netzsch TG 209 F1 microthermal balance in argon. The heating rate of the samples was 10 °C/min, Sample weight was 2-4 mg. Temperature range was 25–600 °C. The error in determining the loss of sample mass was 1·10⁻⁴ mg.

Synthesis

Compound **1-3** (Figure 1) were synthesized by halogenation reaction of pre-synthesized BODIPY **1a-3a**.[20] Synthesis of **2** was described earlier.[39,40] Synthesis of β-dibromodipyrromethene difluoroborate was carried out upon low temperature in tetrahydrofuran environment.[40] The preferred reaction conditions in our investigation were room temperature and dichloromethane environment, which led to a slight increase in the yield of the target product.

5,5'-Dibromo-3,3',4,4'-tetramethyl-2,2'-dipyrromethene difluoroborate (**1**, (α-Br)₂-BODIPY; M=405.87) was synthesized from 3,3',4,4'-tetramethyl-2,2'-dipyrromethene difluoroborate according to reaction:
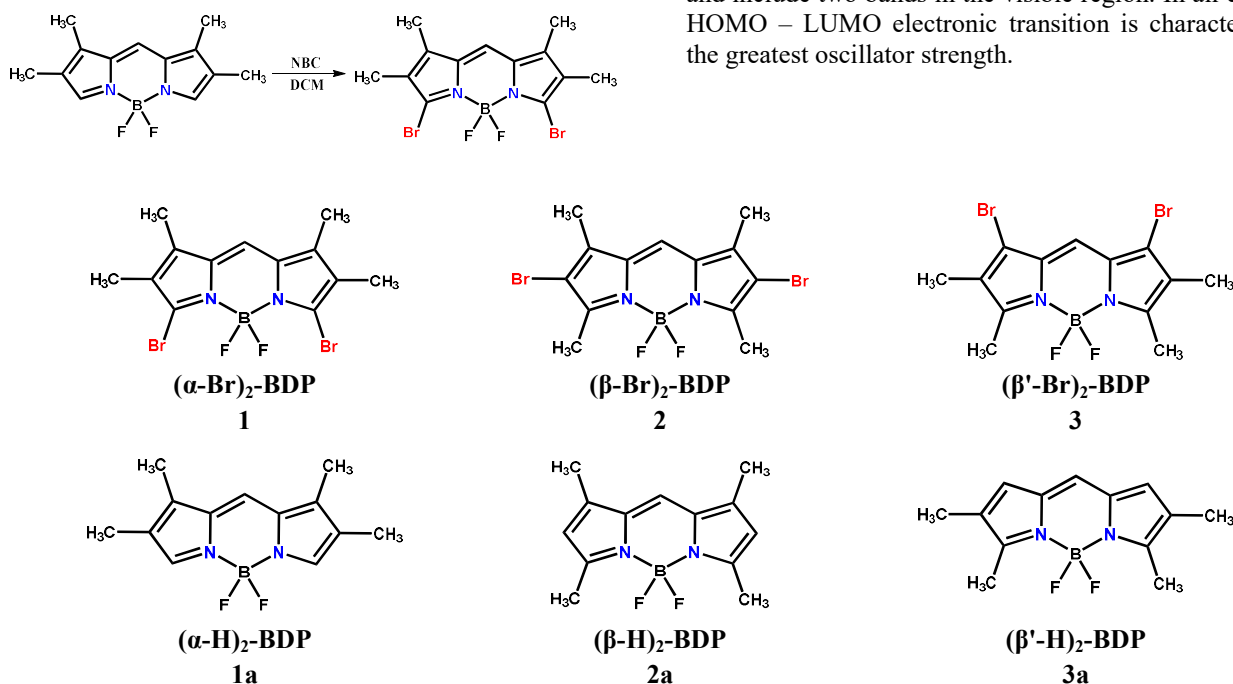

To a solution of 0.1 g (0.403 mmol) of 3,3',4,4'-tetramethyl-2,2'-dipyrromethene difluoroborate in 20 mL of dried CH_2Cl_2 added the solution dropwise of N-bromosuccinimide (0.158 g, 0.887 mmol) in 20 mL of dried dichloromethane. Reaction mixture was stirred at room temperature during 1.5 h. The solution was concentrated at low pressure. The crude product was sorbed by silica gel and purified by column chromatography (hexane:CH_2Cl_2 2:1 mixture). Yield: 0.122 g (0.302 mmol, 75%). Mass spectrum, *m/z*: 406.25 [M+H]⁺. ¹H NMR spectrum (CDCl₃) δ ppm: 7.05 (s, 2H, ms-H); 2.56, 2.47, 2.24, 2.12 (s, 4 × 3H, CH₃).

4,4'-Dibromo-3,3',5,5'-tetramethyl-2,2'-dipyrromethene difluoroborate (**2**, (β-Br)₂-BODIPY; M=405.87) was synthesized similarly from 0.103 g (0.417 mmol) of 3,3',5,5'-tetramethyl-2,2'-dipyrromethene difluoroborate. Yield: 0.152 g (0.375 mmol, 90%). Mass spectrum, *m/z*: 406.08 [*M*+H]⁺. ¹H NMR spectrum (CDCl₃) δ ppm: 7.07 (s, 1H, ms-H); 2.55 (s, 6H, CH₃); 2.27 (s, 6H, CH₃).

3,3'-Dibromo-4,4',5,5'-tetramethyl-2,2'-dipyrromethene difluoroborate (**3**, (β'-Br)₂-BODIPY; M=405.87) was synthesized from 0.061 g (0.247 mmol) 4,4',5,5'-tetramethyl-2,2'-dipyrromethene difluoroborate. Yield 0.077 g (0.191 mmol, 77%). Mass spectrum, *m/z*: 406.35 [M+H]⁺. ¹H NMR spectrum (CDCl₃) δ ppm: 7.15 (s, 1H, ms-H); 2.55 (s, 6H, CH₃); 2.04 (s, 6H, CH₃).

Results and Discussion

Computational modeling

The results of computational modeling are presented in our previous work.[41]

It was established in the series of dibromosubstituted BODIPY bromine atom position does not affect the B–N coordination bond length. Total energy analysis shows that the compounds stability decreases in the series: (β-Br)₂-BDP, (β'-Br)₂-BDP, (α-Br)₂-BDP. Calculated photostability of dibromosubstituted BODIPY decreases in the same series. It is confirmed by a decrease of the energy gap value.

TDDFT spectra of studying compounds **1-3** is typical and include two bands in the visible region. In all cases, the HOMO – LUMO electronic transition is characterized by the greatest oscillator strength.

Figure 1. Research objects **1-3** and comparison compounds **1a-3a**.

HOMO is characterized by delocalization of electron density on BODIPY core and bromine atoms. LUMO is mainly delocalization on the BODIPY core. Comparing HOMO/LUMO localization on bromine atoms it is supposed that (β-Br)$_2$-BDP is characterized by PET, other BODIPY – ICT.[40] Besides in the case of dibromo-BODIPY we can expected by stronger fluorescence quenching due to the increased charge (electron) transfer process efficiency.

Chromophore and fluorescent properties of 1-3 and 1a-3a

Spectral characteristics of BODIPY **1-3** and **1a-3a** are determined in a series of various natures solvents. Quantitative characteristics of EAS and fluorescence spectra of BODIPY **1-3** are presented in Table 1.

Investigating compounds are characterized by two-band absorption spectra typical for BODIPY.[41] Compared to non-brominated complexes **1a-3a**, the intense absorption band maximum of (α-Br)$_2$-BDP (**1**) and (β-Br)$_2$-BDP (**2**) is bathochromically shifted by 5–31 nm, λ$_1$ band maximum of (β'-Br)$_2$-BDP (**3**) is shifted to the blue region up to 3 nm (Figure 2a). This is due to the fact that bromine atoms in α- and β-position of BODIPY pyrrole fragments show positive mesomeric effect (+C) which prevails over the negative

inductive effect (-I). This leads to electron density increase in chromophore molecule. When bromine atoms are substituted for the β', β'-positions, the influence of the +C-mesomeric effect is apparently minimal.

The molar absorption coefficient logarithm of **1-3** S$_0$-S$_1$ band is 4.60–5.16, which is comparable to the extinction coefficient values for BODIPY precursors **1a-3a** (Tables 1, 2). However, it should be noted that molar absorption coefficient value of complex **3** is higher than other studied complexes.

Emission spectra of the compounds **1-3** and **1a-3a** are mirror reflection of their intense absorption band (Figure 2b).[4,20,41] The intense band maximum in the emission spectra of BODIPY **1–3** lies in the 544–558 nm range. Wherein, a bathochromic shift of the intense emission band maximum of bromine BODIPY **1-3** is observed compared to unsubstituted complexes **1a-3a** (Tables 1, 2). The solvent nature does not have a strong effect on the position of the intense emission band maximum of Br-substituted compounds **1-3**.

Stokes shift value for complexes **1-3** is 306–665 cm^{-1}. These values are higher than for corresponding unsubstituted BODIPY **1a-3a** (Table 2). In polar solvents the shift value is higher compared to nonpolar (Table 1) apparently due to an increase in the contribution of specific interactions to non-radiative energy losses in polar solvents.

Table 1. Quantitative characteristics of EAS and fluorescence spectra of (α-, β-, β'-Br)$_2$-BDP **1-3** in organic solvents.

| Solvent	BODIPY	λ^{abs}_{max}, nm	lgε	λ^{fl}_{max}, nm	$\Delta\nu_{St}$, cm^{-1}
cyclohexane	(α-Br)$_2$-BDP	541; 377	-	554	434
	(β-Br)$_2$-BDP	538; 375	4.83; 4.00	547	306
	(β'-Br)$_2$-BDP	533; 387	5.15; 4.18	544	379
benzene	(α-Br)$_2$-BDP	543; 383	4.97; 3.91	558	495
	(β-Br)$_2$-BDP	533; 380	4.60; 3.57	546	447
	(β'-Br)$_2$-BDP	538; 387	5.15; 4.07	552	471
chloroform	(α-Br)$_2$-BDP	542; 380	4.91; 3.92	556	465
	(β-Br)$_2$-BDP	539; 379	4.65; 3.81	549	338
	(β'-Br)$_2$-BDP	536; 386	5.05; 4.15	550	475
THF	(α-Br)$_2$-BDP	535; 380	4.92; 4.00	551	543
	(β-Br)$_2$-BDP	529; 378	4.87; 3.85	547	622
	(β'-Br)$_2$-BDP	534; 385	4.93; 3.66	546	412
ethanol	(α-Br)$_2$-BDP	534; 377	-	550	545
	(β-Br)$_2$-BDP	528; 377	-	545	591
	(β'-Br)$_2$-BDP	532; 388	4.85; 3.89	546	482
DMF	(α-Br)$_2$-BDP	533; 382	4.94; 4.02	551	613
	(β-Br)$_2$-BDP	528; 378	4.60; 3.77	546	624
	(β'-Br)$_2$-BDP	535; 382	4.73; 3.82	548	443
acetonitrile	(α-Br)$_2$-BDP	532; 384	4.82; 3.94	548	549
	(β-Br)$_2$-BDP	525; 377	4.86; 3.96	544	665
	(β'-Br)$_2$-BDP	531; 382	4.86; 3.58	545	484
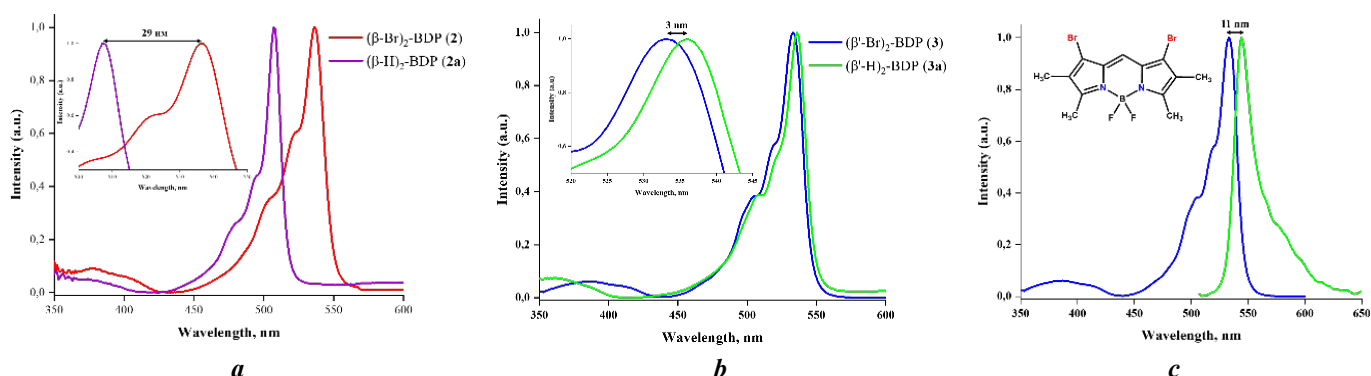
Figure 2. Normalized EAS of **2,3** and **2a,3a** (*a*, *b*); normalized EAS and emission spectra of **3** (*c*) in cyclohexane.

Table 2. Quantitative characteristics of EAS and fluorescence spectra of (α-, β-, β'-H)₂-BDP **1a-3a** in organic solvents.

Solvent	BODIPY	λ^{abs}_{max}, nm	lgε	λ^{fl}_{max}, nm	$\Delta\nu_{St}$, cm⁻¹
cyclohexane	(α-H)₂-BDP	527; 396	4.92; 4.07	539	422
	(β-H)₂-BDP	509; 366	4.96; 3.71	514	191
	(β'-H)₂-BDP	536; 360	4.90; 3.91	549	442
benzene	(α-H)₂-BDP	529; 396	4.76; 3.93	545	555
	(β-H)₂-BDP	509; 366	4.97; 3.69	517	304
	(β'-H)₂-BDP	538; 359	4.83; 3.86	553	504
chloroform	(α-H)₂-BDP	531; 404	4.72; 4.12	542	382
	(β-H)₂-BDP	508; 363	4.95; 3.74	516	305
	(β'-H)₂-BDP	538; 358	4.70; 4.06	553	504
ethanol	(α-H)₂-BDP	522; 399	4.81; 4.10	540	639
	(β-H)₂-BDP	503; 363	4.94; 3.74	512	350
	(β'-H)₂-BDP	533; 358	4.86; 3.92	548	514
DMF	(α-H)₂-BDP	521; 397	4.75; 4.15	-	-
	(β-H)₂-BDP	503; 364	4.88; 3.71	513	388
	(β'-H)₂-BDP	533; 352	4.86; 3.93	549	547

Table 3. Fluorescence and singlet oxygen generation quantitative characteristics of (α-, β-, β'-Br)₂-BDP.

Solvent	BODIPY	Φ_{fl}	$k_r \cdot 10^{-8}$, s⁻¹	$k_{nr} \cdot 10^{-8}$, s⁻¹	τ, ns	Φ_Δ
1	2	3	*4*	*5*	6	7
cyclohexane	(α-Br)₂-BDP	0.66	1.71	0.88	3.87	-
	(β-Br)₂-BDP	0.45	1.69	2.06	2.67	-
	(β'-Br)₂-BDP	0.23	1.43	4.78	1.61	-
benzene	(α-Br)₂-BDP	0.55	1.65	1.35	3.33	0.28
	(β-Br)₂-BDP	0.56	2.37	1.86	2.36	0.32
	(β'-Br)₂-BDP	0.19	1.35	5.74	1.41	0.41
chloroform	(α-Br)₂-BDP	0.58	1.49	1.08	3.89	0.31
	(β-Br)₂-BDP	0.41	1.61	2.32	2.54	0.45
	(β'-Br)₂-BDP	0.18	1.17	5.32	1.54	0.54
ethanol	(α-Br)₂-BDP	0.46	1.34	1.57	3.43	0.50
	(β-Br)₂-BDP	0.32	1.48	3.15	2.16	0.66
	(β'-Br)₂-BDP	0.16	1.38	7.24	1.16	0.72
DMF	(α-Br)₂-BDP	0.31	1.13	2.52	2.74	0.46
	(β-Br)₂-BDP	0.32	1.0	2.13	3.19	0.49
	(β'-Br)₂-BDP	0.11	0.92	7.42	1.20	0.42

1	2	3	4	5	6	7
	$(\alpha\text{-Br})_2$-BDP	0.51	1.62	1.56	3.15	0.49
THF	$(\beta\text{-Br})_2$-BDP	0.44	2.05	2.6	2.15	0.56
	$(\beta'\text{-Br})_2$-BDP	0.20	1.71	6.84	1.17	0.79
	$(\alpha\text{-Br})_2$-BDP	0.38	1.22	1.99	3.11	0.62
acetonitrile	$(\beta\text{-Br})_2$-BDP	0.32	1.75	3.72	1.83	0.67
	$(\beta'\text{-Br})_2$-BDP	0.13	1.35	9.06	0.96	0.75
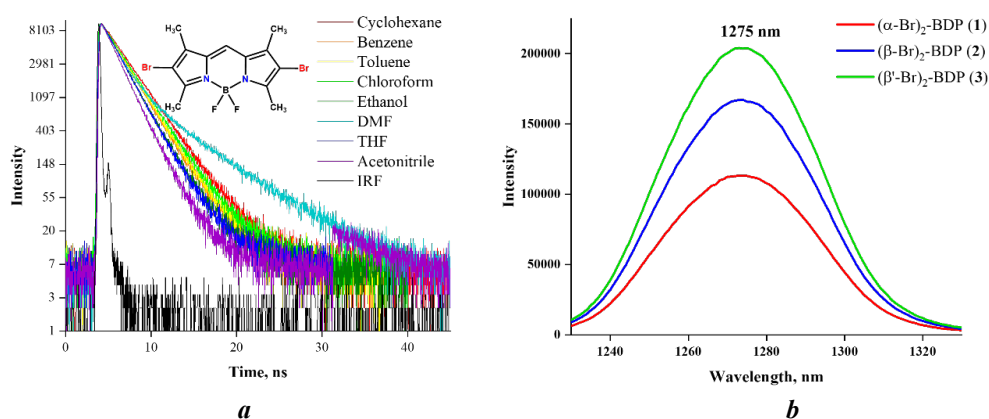
Figure 3. Fluorescence decay curves of **2** (*a*) in organic solvents and $^1O_2$ phosphorescence spectra of **1-3** in chloroform ($\lambda_{ex} = 500$ nm) (*b*)

Table 4. Fluorescence and singlet oxygen generation quantitative characteristics of $(\alpha\text{-}, \beta\text{-}, \beta'\text{-H})_2$-BDP

Solvent	BODIPY	Φ_{fl}	$k_r \cdot 10^{-8}$, s^{-1}	$k_{nr} \cdot 10^{-8}$, s^{-1}	τ, ns	Φ_Δ
	$(\alpha\text{-H})_2$-BDP	0.71	1.16	0.47	6.11	-
cyclohexane	$(\beta\text{-H})_2$-BDP	1.00	1.91	0	5.23	-
	$(\beta'\text{-H})_2$-BDP	0.85	1.38	0.24	6.14	-
	$(\alpha\text{-H})_2$-BDP	0.68	1.18	0.56	5.75	0.14
benzene	$(\beta\text{-H})_2$-BDP	0.88	1.91	0.26	4.60	0.03
	$(\beta'\text{-H})_2$-BDP	0.85	1.58	0.28	5.37	0.03
	$(\alpha\text{-H})_2$-BDP	0.57	0.97	0.73	5.87	0.22
chloroform	$(\beta\text{-H})_2$-BDP	0.90	1.73	0.19	5.21	0.03
	$(\beta'\text{-H})_2$-BDP	0.89	1.37	0.17	6.48	0.02
	$(\alpha\text{-H})_2$-BDP	0.60	0.98	0.65	6.13	0.40
ethanol	$(\beta\text{-H})_2$-BDP	0.88	1.63	0.22	5.39	0.10
	$(\beta'\text{-H})_2$-BDP	0.76	1.13	0.36	6.74	0.08
	$(\alpha\text{-H})_2$-BDP	-	-	-	5.76	0.20
DMF	$(\beta\text{-H})_2$-BDP	0.99	1.99	0.02	4.97	0.10
	$(\beta'\text{-H})_2$-BDP	0.79	1.27	0.34	6.23	0.06
	$(\alpha\text{-H})_2$-BDP	-	-	-	5.91	0.30
THF	$(\beta\text{-H})_2$-BDP	-	-	-	5.05	0.07
	$(\beta'\text{-H})_2$-BDP	-	-	-	6.23	0.07

Fluorescence and singlet oxygen quantum yields of 1-3 and 1a-3a

Obtained results analysis showed that for dibromo-substituted compounds **1-3** the significant dependence of the fluorescence quantum yield on the bromine atoms posi-tion is observed. Fluorescence quantum yield (Φ_{fl}) decrease from 0.66 to 0.11 (Table 3) in the series $(\alpha\text{-Br})_2$-BDP, $(\beta\text{-Br})_2$-BDP, $(\beta'\text{-Br})_2$-BDP. The presence of bromine atoms in BODIPY molecule leads to fluorescence quenching of **1-3** compared to unsubstituted analogues **1a-3a** for which fluo-rescence quantum yield reaches 0.99 (Table 4).

Fluorescence lifetime of dibromo-BODIPY reaches 3.87 ns. The highest lifetime values are observed for (α-Br)$_2$-BDP, which is almost 2 times higher than for (β'-Br)$_2$-BDP. For all compounds τ decrease is observed when moving from non-polar solvents to polar ones. For brominated complexes lifetime is 1.5–5 times lower than for corresponding unsubstituted compounds **1a-3a**. Calculated values of k_r and k_{nr} for **1-3** depend more on the compound structure than on the solvent nature. Br$_2$-BDP exhibits a correlation between bromine atoms positions and k_{nr} value which increases in the series (α-Br)$_2$-BDP, (β-Br)$_2$-BDP, (β'-Br)$_2$-BDP. Fluorescence decay curves are presented in Figure 3a.

Brominated complexes **1-3** are capable of generating singlet oxygen (^{1}O$_2$) (Tables 3, 4). The highest intensity of singlet oxygen generation is observed in chloroform solution (Figure 3b). Experimental results demonstrate a significant singlet oxygen generation for BODIPY **1a** without bromine atoms (from 14 to 40%), which is not typical for such compounds. This issue requires separate study.

Two bromine atoms introduction into compounds **1-3** molecule leads to an increase of singlet oxygen quantum yield up to 0.79 (Table 3, Figure 4) compared to mono-bromosubstituted BODIPY.[41] Φ_Δ values of dibromo-substituted complexes increases in the series (α-Br)$_2$-BDP, (β-Br)$_2$-BDP, (β'-Br)$_2$-BDP (Figure 3b). Similar changes were observed in the work,[40] where Φ_Δ determined by a chemical method using diphenylisobenzofuran (DPBF) was 0.71 in acetonitrile and 0.66 in THF. From a comparison of these results with the data in Table 3 it follows (Φ_Δ 0.67 and 0.56 for CH$_3$CN and THF, respectively), that the values of the singlet oxygen quantum yield determined by the "chemical trap" method turn out to be somewhat overestimated in comparison with similar data obtained by characteristics of phosphorescence at 1275 nm.

There are results of determining Φ_Δ for similar BODIPY with a phenyl group in the *meso*-position[42,43] which were 0.45 in toluene solution and 0.205 in dichloromethane environment. Comparing the data cited above and those obtained by us, it can be assumed that the phenyl fragment introduction into the *meso*-position of dibromo-BODIPY reduces the singlet oxygen quantum yield.

From the presented results it follows that (α-Br)$_2$-BDP and (β-Br)$_2$-BDP can be considered as theranostics with a predominant function of a biovisualizer, and (β'-Br)$_2$-BDP exhibits a photosensitizer function to a greater extent.

Photostability of BODIPY 1-3 and 1a-3a

The kinetic stability of dyes, pigments and luminophores under the influence of intense lighting, in particular UV irradiation in the presence of atmospheric oxygen, is one of the key characteristics of the feasibility of their use in solving practical problems. Numerous spectral measurements have shown that BODIPY **1-3**, like **1a-3a**, are stable under diffuse illumination in solutions. However, under UV irradiation they, like many other chromophores, are subject to discoloration at different rates, depending on the structural features of the molecule.[20,44,45]

Most of the chromophores destruction processes caused by the influence of absorbed light quanta are based on photooxidation reactions with oxygen.[44,46,47]
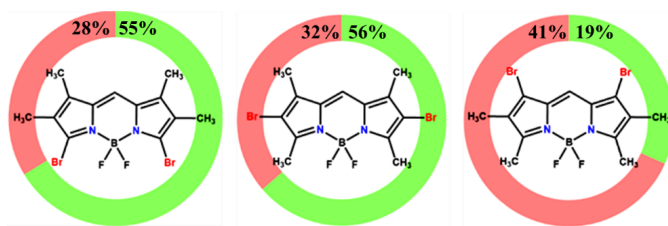

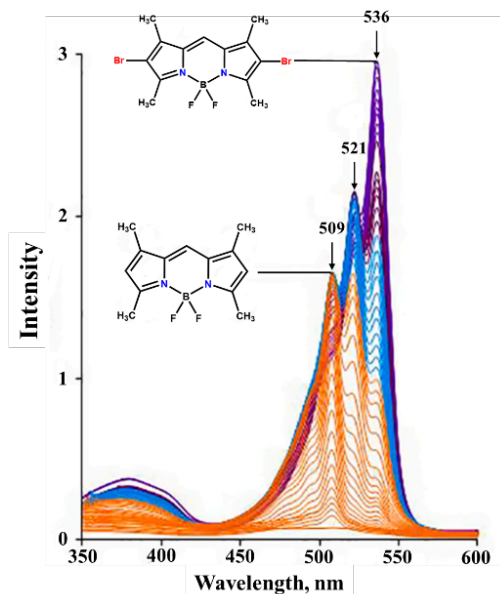**Figure 4.** Fluorescence quantum yield (green) and singlet oxygen quantum yield (red) ratio of Br$_2$-BDP in benzene.

Figure 5. Changes in EAS of solution **β-H-BDP (2a)** and **(β-Br)$_2$-BDP (2)** in cyclohexane[38] under UV irradiation (λ=365 nm).

Characteristic changes in the EAS during the photodestruction of the studied compounds in solutions under UV irradiation are presented in Figure 5.
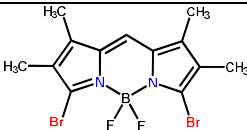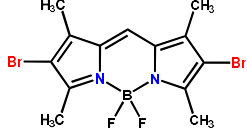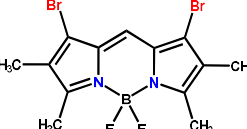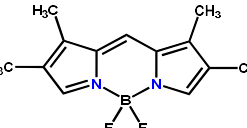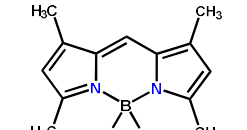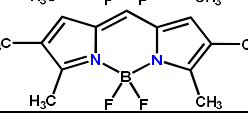
Observed photooxidation rate constants (k_{obs}) of dibromosubstituted complexes **1-3** and the half-life ($t_{1/2}$) of boron(III) dipyrromethenates are presented in Table 5. Molecular structure features of the compounds **1-3** determine their $t_{1/2}$ values in cyclohexane from 17 to 128 hours under chosen experimental conditions.

For bromine substituted boron(III) dipyrromethenates the phototransformation process probably begins with the dehalogenation stage (Figure 5) followed by the destruction of the dye aromatic backbone at the most active centers (methine bridge and nitrogen atoms of the coordination center).[38]

Observed photooxidation rate constants (Table 5) of **1-3** in cyclohexane is slightly higher, the half-life is lower for bromine substituted compounds compared to unsubstituted compounds **1a-3a**, and the compounds halogenated at the β,β- and β',β'-positions **2** and **3** are very close in this characteristic.

As mentioned above, an increase in the electron density in the conjugated dipyrromethene system due to bromine atoms should lead to its increase in the meso-spacer and nitrogen atoms of the pyrrole rings, which favors red-ox reactions at these groups and atoms.

Table 5. Photodestruction process quantitative characteristics of dibromosubstituted BODIPY and their unsubstituted analogues in organic solvents.

No.	BODIPY	Cyclohexane		Benzene	
		$k_{obs} \cdot 10^6$, s^{-1}	$t_{1/2}$, h	$k_{obs} \cdot 10^6$, s^{-1}	$t_{1/2}$, h
1		8.4±0.5	17.2	4.1±0.7	35.7
2		3.4±0.5	38.9	1.2±0.2	128.5
3		3.1±0.3	42.0	2.8±0.3	49.1
1a		6.0±0.6	21.5	4.4±0.9	23.6
2a		2.9±0.3	45.0	3.7±0.4	37.4
3a		3.5±0.2	39.0	4.0±0.4	34.0
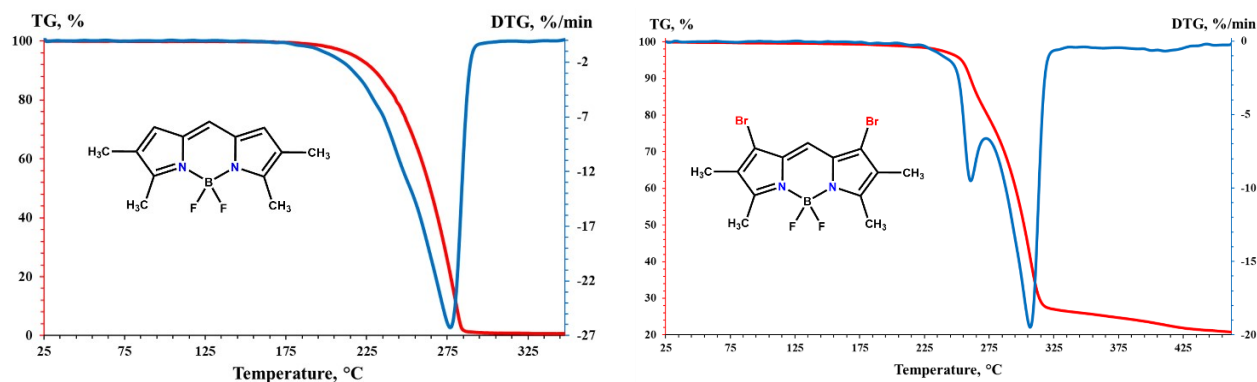
Figure 6. TG and DTG curves of the complexes **3** and **3a.**

In aromatic benzene prone to π-π interactions with dipyrromethenates compound **1-3** demonstrate the increase in photostability compared to cyclohexane. This may be due to the transfer of electron density in the excited state from the chromophore molecule to the solvent molecule. However, this issue requires separate study.

Thermal stability in condensed phase

Besides spectral and fluorescent characteristics the thermal stability of boron(III) dipyrromethenates over a wide temperature range is of great importance for their practical applications. Destruction of the complexes **1-3** and **1a-3a** in the inert atmosphere of argon occurs mainly due to the intramolecular oxidation process intensity of which depends on the dipyrromethenate molecule structure.

The thermal decomposition onset for BODIPY **1-3** and **1a-3a** is displayed on the thermograms in the form of high-speed sample loss weight. Unlike the reference compounds, the thermal destruction of bromine substituted BODIPY includes two stages of sample weight loss (Figure 6). At the first stage, the "separation" of bromine atoms in the form of HBr supposedly occurs. Then the destruction of the dipyrromethene skeleton occurs.

In the thermograms of compounds **1-3** this is displayed as a separate peak at temperatures below the maxi-

mum exo-effect (Figure 6). Brominated complexes (α-Br)₂-BDP and (β-Br)₂-BDP inferior in thermal stability to their non-brominated analogues **1a** and **2a** by 32 °C and 21 °C, respectively (Table 6).

In the case of BODIPY **3** bromine atoms presence in the molecule causes a slight (4 °C) increase in thermal stability compared to **3a**.

Table 6. Thermal properties of BODIPY **1-3** and **1a-3a.**

Compound	T_{start}, °C	T_{max}, °C	T_{end}, °C
(α-Br)₂-BDP (1)	224	325	358
(β-Br)₂-BDP (2)	238	302	310
(β'-Br)₂-BDP (3)	251	307	425
(α-H)₂-BDP (1a)	256	274	423
(β-H)₂-BDP (2a)	259	301	311
(β'-H)₂-BDP (3a)	247	277	285

Aggregation behavior of bromine substituted boron(III) dipyrromethenates in water-organic media

The hydrophobicity and tendency to aggregation of BODIPY molecules in physiological media is one of the problems of their possible practical use in biomedicine. In this case we estimated the aggregation behavior of bromine substituted complexes **1-3** in a mixed solvent THF-water.

It was previously established that tetramethyl substituted BODIPY **2a** aggregates poorly in organic media in the presence of water.[48] The introduction of CH₃ groups into the β-positions of pyrrole fragments leads to an increase in the complex hydrophobicity and intensive formation of H-type aggregates at a volumetric water content (f_w) above 70% due to increased π-π interactions and parallel molecules.[48, 49] The study of the dibromo-substituted boron(III) dipyrromethates aggregation behavior showed that the introduction of two bromine atoms does not lead to a change in the type of aggregates formed in the media with excess water content. Significant changes in EAS and emission spectra of **1-3** is observed under f_w > 70%: strong (up to 61 nm) hypsochromic shift of the intense absorption band maximum, broadening the spectrum profile, significant reduction in absorption efficiency (Figure 7a). Wherein almost complete fluorescence quenching (Figure 7b).

The chromophore concentration increases in the mixture with maximum water content (f_w = 95%) does not lead to any changes, and increase in the intensity of the first band maximum in the EAS (Figure 8) is the most likely associated with an increase in the aggregation intensity and the formation of larger aggregates, wherein the strong fluorescence quenching is observed. Aggregation occurs quickly and significant changes in the spectral characteristics are observed the very next day.

Thus, bromine substituted BODIPY are characterized by high aggregation intensity in the media with water content above 70% with the non-fluorescent H-aggregates formation. To increase the solubility of BODIPY in water-organic media and to avoid aggregation processes, biocompatible nanosized carriers are needed. Further research will be aimed at solving this particular problem.
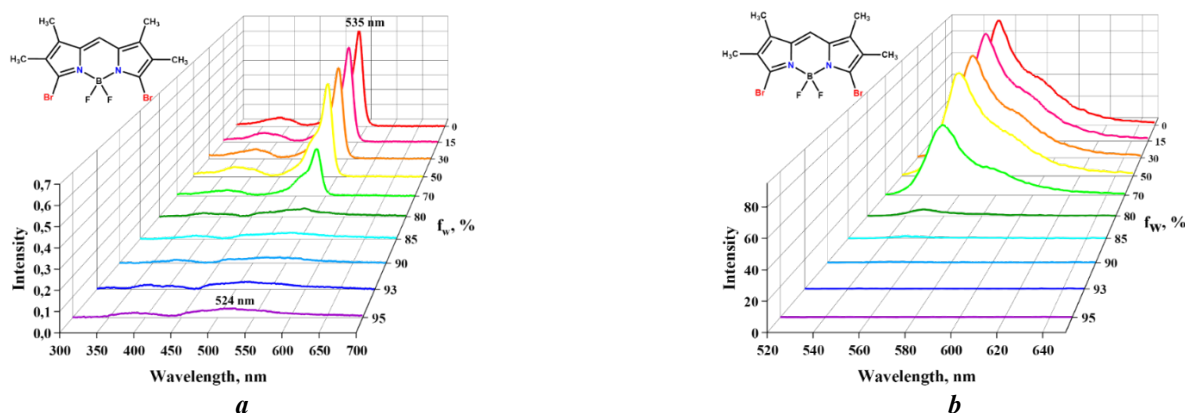

Figure 7. EAS (*a*) and emission spectra (*b*) of (α-Br)₂-BDP (**1**) in the mixture THF-water at constant complex concentration (C_{BDP} ≈ 7 μM) and varying water content (f_w).
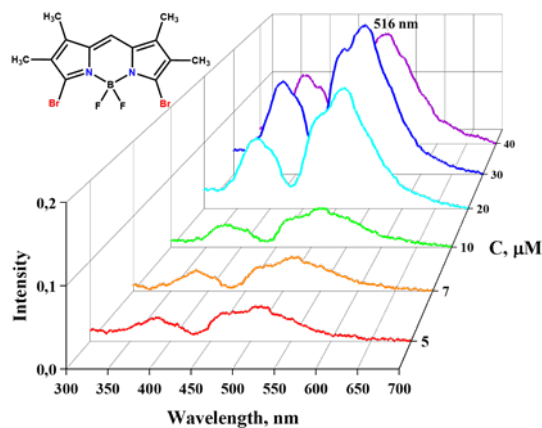

Figure 8. EAS of (α-Br)₂-BDP (**1**) in the mixture THF-water at varying complex concentration from 5 to 40 μM and f_w = 95%.

Conclusions

Quantum chemical modeling of molecules showed that the presence of two bromine atoms in the BF_2-dipyrromethene molecule does not lead to significant changes in the structural and energetic characteristics of the complexes.

Dibromosubstituted BODIPY are characterized by bathochromic (1–8 nm) shift of the maximum of first absorption band compared to analogues without halogen atoms; the transition from nonpolar to polar media shifts λ_1 in the EAS of dibromosubstituted complexes to the blue region; the introduction of bromine atoms into the molecule quenches the fluorescence, but enhances singlet oxygen generation intensity of BODIPY in the series (α-Br)$_2$-BDP, (β-Br)$_2$-BDP, (β'-Br)$_2$-BDP; (α-Br)$_2$-BDP and (β-Br)$_2$-BDP can be considered as theranostics with a predominant function of a biovisualizer, and (β'-Br)2-BDP exhibits a photosensitizer function to a greater extent.

Bromination of BODIPY molecule has a little effect on photo- and thermal stability compared to unsubstituted analogues.

Studied bromine substituted boron(III) dipyrromethenates are characterized by formation of H-aggregates in mixed solvent THF-water at water content in mixture above 70%.

Further research will be aimed at finding ways to introduce Br-BODIPY into biocompatible nanostructured carriers (metal organic frameworks), which will likely significantly increase their solubility in aqueous media.

Author Contributions. Sofya A. Dogadaeva: validation, formal analysis, investigation, visualization. Alexander A. Kalyagin: investigation, formal analysis. Alexander A. Ksenofontov: investigation, formal analysis. Lubov A. Antina: writing - review & editing, funding acquisition, conceptualization. Mikhail B. Berezin: methodology, conceptualization, writing - original draft. Elena V. Antina: conceptualization, writing - review & editing, supervision. Alexander S. Semeikin: methodology.

References

1. a) *Handbook of Porphyrin Science: With Applications to Chemistry, Physics, Materials Science, Engineering, Biology and Medicine* (Kadish K.M., Smith K.M., Guilard R., Eds.), Vols. 1-46, ISSN: 1793–9518; b) Berezin B.D. *Coordination Compounds of Porphyrins and Phthalocyanines*. New York: Brisbane, Toronto, **1981**. 299 p.
2. Koifman O.I., Ageeva T.A., Beletskaya I.P. *et al. Macroheterocycles* **2020**, *4*, 311–467, doi: 10.6060/mhc200814k.
3. Falk H. The Chemistry of Linear Oligopyrroles and Bile Pigments. Vienna: Springer, **1989**.
4. a) Antina E.V., Berezin M.B., V'yugin A.I. *Russ. J. Inorg. Chem.* **2022**, *67*, 321–337, doi: 10.1134/S0036023622030032; b) Vashurin A.S., Boborov A.V., Botnar A.A., *et al. ChemChemTech* **2023**, *66*(7), 76–97, doi: 10.6060/ivkkt.20236607.6840j.
5. Martynov V.I., Pakhomov A.A. *Russ. Chem. Rev.* **2021**, *90*, 1213–1262, doi: 10.1070/RCR4985.
6. Gui R., Jin H., Bu X. *Coord. Chem. Rev.* **2019**, *383*, 82–103, doi: 10.1016/j.ccr.2019.01.004.
7. Ni Y., Wu J. *Org. Biomol.Chem.* **2014**, *12*, p. 3774–3791, doi: 10.1039/C3OB42554A.
8. Kowada T., Maeda H., Kikuchi K. *Chem. Soc. Rev.* **2015**, *44*, 4953–4972, doi: 10.1039/C5CS00030K.
9. Cheng H.-B., Cao X., Zhang S. *Adv. Mater. (Deerfield Beach, Fla.)* **2023**, *35*, e2207546, doi: 10.1002/adma.202207546.
10. Boens N., Leen V., Dehaen W. *Chem. Soc. Rev.* **2012**, *41*, 1130–1172, doi: 10.1039/C1CS15132K.
11. Zhang W., Ahmed A., Cong H. *Dyes Pigm.* **2021**, *185*, 108937, doi: 10.1016/j.dyepig.2020.108937.
12. Turksoy A., Yildiz D., Akkaya E.U. *Coord. Chem. Rev.* **2019**, *379*, 47–64, doi: 10.1016/j.ccr.2017.09.029.
13. Lin G., Hu M., Zhang R. *J. Med. Chem.* **2021**, *64*, 18143–18157, doi: 10.1021/acs.jmedchem.1c01643.
14. Poddar M., Misra R. *Coord. Chem. Rev.* **2020**, *421*, 213462, doi: 10.1016/j.ccr.2020.213462.
15. Bobrov A.V., Kishalova M.V., Merkushev D.A., Marfin Y.S. *J. Phys.: Conf. Ser.* **2021**, *1822*, 12020, doi: 10.1088/1742-6596/1822/1/012020.
16. Gupta M., Mula S., Ghanty T.K. *J. Photochem. Photobiol., A* **2017**, *349*, 162–170, doi: 10.1016/j.jphotochem.2017.09.033.
17. Solomonov A.V., Marfin Y.S., Rumyantsev E.V. *Dyes Pigm.* **2019**, *162*, 517–542, doi: 10.1016/j.dyepig.2018.10.042.
18. Squeo B.M., Ganzer L., Virgili T., Pasini M. *Molecules* **2020**, *26*, 153, doi: 10.3390/molecules26010153.
19. Bañuelos J. *The Chemical Record* **2016**, *16*, 335–348, doi: 10.1002/tcr.201500238.
20. Berezin M.B., Dogadaeva S.A., Antina E.V. *Dyes Pigm.* **2022**, *202*, 110215, doi: 10.1016/j.dyepig.2022.110215.
21. Guseva G.B., Lukanov M.M., Ksenofontov A.A. *J. Photochem. Photobiol., A* **2023**, *444*, 114926, doi: 10.1016/j.jphotochem. 2023.114926.
22. Frisch M.J., Trucks G.W., Schlegel H.B., Scuseria G.E., Robb M.A., Cheeseman J.R., Scalmani G., Barone V., Petersson G.A., Nakatsuji H., Li X., Caricato M., Marenich A.V., Bloino J., Janesko B.G., Gomperts R., Mennucci B., Hratchian H.P., Ortiz J.V., Izmaylov A.F., Sonnenberg J.L., Williams-Young D., Ding F., Lipparini F., Egidi F., Goings J., Peng B., Petrone A., Henderson T., Ranasinghe D., Zakrzewski V.G., Gao J., Rega N., Zheng G., Liang W., Hada M., Ehara M., Toyota K., Fukuda R., Hasegawa J., Ishida M., Nakajima T., Honda Y., Kitao O., Nakai H., Vreven T., Throssell K., Montgomery J.A., Jr., Peralta J.E., Ogliaro F., Bearpark M.J., Heyd J.J., Brothers E.N., Kudin K.N., Staroverov V.N., Keith T.A., Kobayashi R., Normand J., Raghavachari K., Rendell A.P., Burant J.C., Iyengar S.S., Tomasi J., Cossi M., Millam J.M., Klene M., Adamo C., Cammi R., Ochterski J.W., Martin R.L., Morokuma K., Farkas O., Foresman J.B., and Fox D.J. Gaussian, Inc., Wallingford CT, **2019**, https://gaussian.com/gaussian16/.
23. Dunning T.H. *J. Chem. Phys.* **1989**, *90*, 1007–1023, doi: 10.1063/1.456153.
24. Chai, J.-D. Head-Gordon M. *J. Chem. Phys.* **2008**, *128*, 84106, doi: 10.1063/1.2834918.
25. Yanai T., Tew D.P., Handy N.C. *Chem. Phys. Lett.* **2004**, *393*, 51–57, doi: 10.1016/j.cplett.2004.06.011.
26. Takano Y., Houk K.N. *J. Chem. Theory Comput.* **2005**, *1*, 70–77, doi: 10.1021/ct049977a.
27. Andrienko G.A. *Chemcraft - graphical software for visualization of quantum chemistry computations*. Version 1.8, build 682. https://www.chemcraftprog.com
28. Lakowicz J.R. *Principles of Fluorescence Spectroscopy*. New York: Springer, **2006**. 954 p.

29. Antina L.A., Bumagina N.A., Kalinkina V.A. *Spectrochim. Acta, Part A* **2022**, *278*, 121366 doi: 10.1016/j.saa.2022.121366.

30. Antina L.A., Kalyagin A.A., Ksenofontov A.A. *J. Mol. Liq.* **2021**, *337*, 116416, doi: 10.1016/j.molliq.2021.116416.

31. Antina L.A., Kalyagin A.A., Ksenofontov A.A. *Spectrochim. Acta, Part A* **2022**, *265*, 120393, doi: 10.1016/j.saa.2021.120393.

32. Mchiri C., Dhifaoui S., Ezzayani K. *Polyhedron* **2019**, *171*, 10–19, doi: 10.1016/j.poly.2019.06.055.

33. Taguchi D., Nakamura T., Horiuchi H. *J. Org. Chem.* **2018**, *83*, 5331–5337, 10.1021/acs.joc.8b00782.

34. Demirbaş Ü., Pişkin M., Akçay H.T. *Synth. Met.* **2017**, *223*, p. 166–171, doi: 10.1016/j.synthmet.2016.12.004.

35. Wilkinson F., Helman W.P., Ross A.B. *J. Phys. Chem. Ref. Data* **1993**, *22*, 113–262, doi: 10.1063/1.555934.

36. Pellosi D.S., Tessaro A.L., Moret F. *J. Photochem. Photobiol., A* **2016**, *314*, 143–154, doi: 10.1016/j.jphotochem.2015.08.024.

37. Chen P., Sun S., Hu Y. *Dyes Pigm.* **1999**, *41*, 227–231, doi: 10.1016/S0143-7208(98)00088-6.

38. Nuraneeva E.N., Guseva G.B., Antina E.V., V'yugin A.I. *J. Photochem. Photobiol., A* **2022**, *426*, 113789, doi: 10.1016/j.jphotochem.2022.113789.

39. Antina L.A., Ravcheeva E.A., Dogadaeva S.A. *J. Photochem. Photobiol., A* **2024**, *449*, 115370, doi: 10.1016/j.jphotochem.2023.115370.

40. Hu W., Zhang R., Zhang X.-F. *Spectrochim. Acta, Part A* **2022**, *272*, 120965, doi: 10.1016/j.saa.2022.120965.

41. Dogadaeva S.A., Antina L.A., Ksenofontov A.A. *J. Mol. Liq.* **2023**, *382*, 121892, doi: 10.1016/j.molliq.2023.121892.

42. Gorbe M., Costero A.M., Sancenón F. *Dyes Pigm.* **2019**, *160*, 198–207, doi: 10.1016/j.dyepig.2018.08.007.

43. Zhang X.-F., Yang X. *J. Phys. Chem., B* **2013**, *117*, 5533–5539, doi: 10.1021/jp4013812.

44. Berezin M.B., Antina E.V., Guseva G.B. *Inorg. Chem. Commun.* **2020**, *111*, 107611, doi: 10.1016/j.saa.2022.120965.

45. Kritskaya A.Y., Berezin M.B., Antina E.V., Vyugin A.I. *J. Fluoresc.* **2019**, *29*, 911–920, doi: 10.1007/s10895-019-02403-2.

46. Berezin D.B., Likhonina A.E., Serov I.N., Andrianov V.G. *Russ. J. Gen. Chem.* **2017**, *87*, 979–984, doi: 10.1016/j.inoche.2019.107611.

47. Kautsky H. *Trans. Faraday Soc.* **1939**, *35*, 216, doi: 10.1039/TF9393500216.

48. Descalzo A.B., Ashokkumar P., Shen Z., Rurack K. *ChemPhotoChem* **2020**, *4*, 120–131, doi: 10.1002/cptc.201900235.

49. Antina L.A., Ksenofontov A.A., Kazak A.V. *Colloids Surf., A* **2021**, *618*, 126449, doi: 10.1016/j.colsurfa.2021.126449.